BNL-62714

TARGET DESIGNS FOR THE BROOKHAVEN NATIONAL LABORATORY 5-MW PULSED SPALLATION NEUTRON SOURCE*

Hans Ludewig, Michael Todosow and James R. Powell
Department of Advanced Technology
Brookhaven National Laboratory
Upton, New York 11973

INTRODUCTION

A feasibility study of a compact high power density target for a spallation neutron source was under-taken. The target arrangement consists primarily of heavy metal, with appropriate cooling passages. A high intensity proton beam of intermediate energy is directed at the target, where it interacts with the heavy metal nuclei. The subsequent spallation reactions produce several neutrons per proton resulting in an intense neutron source. The proton beam is assumed to have an energy of 5 MW, and to be cyclic with a repetition rate of 10Hz and 50Hz.

The study was divided into two broad sections. First, an analysis of preliminary target designs was undertaken to ensure the overall feasibility of the concepts involved in the design and eventual construction of such a high power density target. Second, two proposed target designs, based on the first set of analyses, are investigated in more detail. Special care is taken to ensure that the neutron fluxes in the moderator are at the desired level, no material compatibility problems exist, and the target is able to operate in a reliable and safe manner.

Several target materials, coolant types, and target arrangements are investigated in the first section. The second section concentrates on a single target material and geometric arrangement. However, several structural material choices continue to be investigated with the aim of minimizing the effects of structural heating, and associated thermally induced stresses. In the final section the conclusions of this preliminary study are summarized.

DESIGN AND ANALYSIS OF PRELIMINARY TARGETS

Several combinations of target geometry, materials and coolant types were initially investigated in order to gain experience regarding the feasibility of designing a target which would operate with a maximum beam power of 5MW. These investigations took the form of physics calculations of full density cylindrical heavy metal targets. The metals chosen were tungsten and uranium-238 embedded in a light water reflector. Proton beam energies of 1 GeV and 10 GeV were used in these studies, implying steady-state beam currents of 5.0 and 0.5 mA, respectively. The fluid dynamics and heat transfer investigations considered the following options, as given in Table 1.

Table 1
Preliminary Geometry and Coolant Combinations

Geometry	Coolant		
Rods (Axial)*	Helium	Sodium	Lead
Particle Bed (Radial)#		Sodium	Lead

* Arranged along direction of proton beam.
\# Arranged at right angles to direction of proton beam.

* This work was performed under the auspices of the U.S. Department of Energy.

In carrying out the fluid dynamics and heat transfer analyses it was assumed that the power was deposited uniformly in the target, that the length was equivalent to 30 cm of solid target material, and that all of the beam power (5MW) was deposited in the target.

NUCLEAR ANALYSES

The nuclear analyses for proposed targets were carried out using the LAHET Code System (LCS) which simulates the interaction of the incident proton beam with the target constituents, predicts the particles and product nuclei that are produced, and then follows the particles through subsequent transport and interactions until they are absorbed or leak from the system. In addition, these predictions eventually take into account the build-up, burn-out, and decay of nuclei with time, and the impact of these processes on the time-dependent behavior of the system as a whole. The analyses represent only a detailed simulation of the system at essentially t=0.0; time-dependent characteristics will not be considered in this design phase. (Some time-dependent aspects are addressed in a companion paper [Ludewig, 1996]).

The major outputs required from the nuclear analyses of the target are:

- Flux levels and space and energy-dependent spectra available for experimenters.
- Nuclear heating, both prompt (and eventually decay), for setting cooling requirements, determining material performance, and evaluating accident scenarios/consequences.
- Eventually, isotopic inventories as a function of time to estimate source terms, identify potential materials compatibility problems, and estimate system performance and define operations.

The basic tool is the Los Alamos National Laboratory (LANL) developed LAHET Code System (LCS) which consists of two major modules: 1) LAHET, a modified version of the HETC intranuclear cascade code for evaluations above 20 MeV, and 2) HMCNP, a modified version of the well known MCNP transport code for calculations from 20 MeV down to thermal energies. A number of additional codes are also provided with the LCS to perform linking between modules and post-process the results.

The fact that both LAHET and HMCNP are Monte Carlo codes is of particular significance to the design of the proposed spallation target/moderator configurations. Both codes employ a combinatorial surface/cell specification of the problem geometry which permits modeling of the target configurations with minimal approximations. In addition HMCNP employs nuclear data from the ENDF/B files in essentially unaproximated point-wise form which avoids the complications associated with collapsing the data to a group structure and *a priori* knowledge of the space-energy dependent spectra in the system. In addition, HMCNP utilizes the $S(\alpha,\beta)$ formalism for scattering off the bound moderators, and water molecules in the coolant/reflector. The major limitation of Monte Carlo is the statistical nature of the results; this is inherent to the method, and creates difficulties when localized information is desired. In principle, however, the accuracy of the predictions is limited only by the accuracy of the nuclear data, the detail to which the actual geometry is modeled (which as noted above does not have to conform to the regular meshes required by most deterministic methods), and the number of particle histories considered. This last point is not trivial, however, and typical design calculations place considerable demands on computer resources in terms of running time and storage.

The analyses performed in the initial phase of the study considered a solid metal target of either tungsten or uranium-238, 10 cm. in radius, and surrounded by a 100 cm. thick light water reflector. Figure 1 shows a schematic arrangement of this geometry. The beam spot was assumed to have an area of 1 $cm.^2$, and impinge on one of the flat surfaces of the cylinder. The results of these calculations take the form of neutron/proton (n/p) ratios and the spatial distributions of the neutron flux in the moderator volume. The n/p ratios for the two target materials and two neutron energies are summarized in Tables 2 and 3:

Table 2
n/p ratios for a Tungsten target.

	1GeV	10GeV
Evaporation & Cascade	24.8	247.0
n,xn	1.8	22.5
Total	26.6	269.5

Table 3
n/p ratios for a Uranium-238 target.

	1GeV	10 GeV
Evaporation & Cascade	32.8	319.3
n,xn	1.7	20.6
Fission	11.6	125.2
Total	46.1	465.1

The above results indicate that the number of neutrons produced per proton scales approximately linearly with proton energy. Thus, for the same total beam power it is expected that approximately the same total number of neutrons would be produced, regardless of proton energy within this energy range. The difference between these two cases would manifest itself in the spatial distribution of the neutron flux. The higher energy proton beam would penetrate deeper into the target and thus the neutron flux profile would be expected to be flatter, compared to the profile resulting from a lower energy proton beam.

The uranium-238 target produces approximately twice the neutron flux of the tungsten target. This increase for the uranium target is due to the extra neutrons produced by fission. Both targets would parasitically absorb a significant fraction of the neutrons which leak back into the target following slowing down in the moderator, since both have significant neutron absorption cross sections.

FLUID DYNAMICS AND HEAT TRANSFER ANALYSIS

Fluid dynamics and heat transfer analyses were carried out for the selected combinations described in Table 1. Based on the physics results it was decided to concentrate on a target using tungsten as the heavy metal. This decision was based on the elimination of fission products, which was felt to be more important than the higher flux possible with uranium-238. Furthermore, tungsten has the advantage of an extremely high melting point, which will enhance the safety in case of an over heating malfunction, in addition to having demonstrated performance as a spallation target in LANSCE. In order to develop a specific design the physics results developed above for 1GeV protons with a total beam energy of 5MW was assumed. Examination of the spatial distributions calculated above shows that the bulk of the neutrons are produced in the first 30 cms. of the target. Thus, a target length equivalent to 30 cms of tungsten was chosen. In order to cool the target it must be arranged with sufficient cooling passages. Two arrangements were considered at this preliminary stage.

First, a configuration consisting of rods arranged in a hexagonal pattern was considered. The rod pitch/diameter ratio was chosen in such a manner as to yield an overall tungsten density of approximately 80%. To compensate for the lower density the target length was increased to 37.5 cm. Assuming that the rods are 5.0 mm in diameter, the desired pitch is 5.3 mm. A total of 127 rods are used in the target, resulting in an outside diameter of 6.89 cm.

The second configuration consists of a particle bed of tungsten spheres randomly packed in a co-axial volume formed by two porous tubes (frits). Since randomly packed spheres have an average void fraction of approximately 35%, the length of the cylinder is required to be 47.0 cms. The outside cylinder is assumed to be 7.0 cm in diameter, and the inside cylinder diameter is set by fluid dynamic considerations. The tungsten spheres will be assumed to be 2.0 mm. in diameter.

In the rod target, inlet coolant flows axially along the annular channel formed by the outside of the heavy metal target and the pressure vessel. Before entering the target the coolant cools the window. It enters the target at the same end at which the proton beam enters the target, flows axially along the rods, and out the far end. The coolant leaves the target volume through a co-axial feed pipe. In all the target configurations three coolants were considered i.e. gaseous helium, liquid sodium, and liquid lead. In the case of the particle bed target, the coolant enters in a plenum in front of the window and then flows axially through an annular volume cooling the pressure vessel. Finally, it turns and enters another annular plenum surrounding a frit, which feeds the packed bed of tungsten particles. The coolant flows radially through the bed, and then axially out of the target. Only lead and sodium will be considered as coolants in this case, since the outlet duct will be a streaming path in the case of helium.

The preliminary results for the rod target indicate that in every case a compromise must be made, and it is clear that further analysis is required. In the case of the helium cooled target it is clear that operating pressure, exit temperature, and the exit velocity have not been optimized. It might be necessary to increase the pressure in order to reduce the exit velocity. However, this would increase the pressure vessel wall thickness, increasing the neutron parasitic absorption. The shortcomings of the lead cooled target are directly attributable to the relatively low value of specific heat and relatively high melt temperature. Since the outlet temperature

is being limited to values between 800K and 900K a relatively high liquid lead mass flow rate is required to cool the target, implying a high pressure drop. Thus, although liquid metal cooled systems generally operate at low pressures this is not the case with lead in this particular application. Finally, in the case of a sodium cooled target a reasonable compromise seems possible. However, the use of sodium in close proximity to hydrogenous moderators will pose facility safety problems. This fact might eliminate sodium as a possible coolant for the proposed design.

It appears that many of the difficulties associated with a liquid lead cooled rod target array can be eliminated by adopting the radial flow particle bed type design. Finally, it should be pointed out that if lead is chosen as the coolant it will also become part of the neutron producing medium. Thus the 47 cm. long column of lead forming the outlet duct will not only act as an efficient proton shield, but also as a viable neutron source

PRELIMINARY DESIGN AND ANALYSIS OF THE PROPOSED TARGETS

The exploratory analyses carried out above were used to configure target designs for the BNL spallation source. Based on the above analyses it is clear that the high power densities expected in this target and its cyclic operational mode require that the target include the following features:

1) A large heat transfer area per unit volume, to ensure acceptable metal surface temperatures,
2) A short conduction path length to ensure low cyclic stresses as the proton beam intensity rises and falls,
3) A coolant which can operate at reasonably low pressures and temperatures to ensure that the pressure vessel wall thickness is not excessive. Additionally the coolant should be compatible with an emergency cooling system, and
4) All metal components should have a melt temperature which is as high as possible, to ensure a large temperature margin in the event of an upset condition.

The above requirements can be satisfied most easily by selecting a particle bed type target, and arranging the cooling paths in such a manner that the maximum bed thickness is no more than approximately 5 cm - 10 cm. In addition pressurized heavy water (D_2O) will be used as the coolant. Heavy water would be compatible with light water, which would be used as the emergency coolant, while any of the liquid metals proposed above would not be compatible with light water. Pressurized helium would be compatible with light water, but the required operating pressures in this case would be excessively high. Two target configurations, based on the above conceptual requirements will be outlined below. In the first configuration the particle beds are arranged at right angles to the proton beam, while the second configuration will consist of beds arranged parallel to the beam.

DESCRIPTION OF FIRST TARGET CONFIGURATION

The initial target configuration, which satisfies all the above requirements is shown in Figure 2. The overall dimensions are approximately 15x15x60 cms., with the large dimension in the direction of the proton beam. As can be seen from the Figure, the target consists of a series of particle beds contained between porous plates (frits) arranged at right angles to the direction of the proton beam. The tungsten particles, which are the primary target, are assumed to have a diameter of 500 microns. In the present investigation tungsten, stainless steel, beryllium, and aluminum will be considered as possible frit materials. Furthermore, it is seen that the coolant passages are arranged in such a manner that a single inlet plenum feeds alternate frit pairs, while the other frit pairs feed the single outlet duct. In this manner any of the frit-particle bed-frit combinations (also known as elements) can be varied in thickness in the direction of the beam to optimize neutron production, leakage, energy deposition, cooling requirements, and mechanical considerations. The target is expected to operate in a pulsed mode (10Hz and 50Hz.) with a proton beam energy of 3.6 GeV and a total beam power of 5 MW.

The coolant will be introduced into the target at a pressure of 5.0 bars and a temperature of 40°C. The frit, particle-bed combination is expected to have a pressure drop of ≈ 1.0 bar. Thus, from fluid property tables it can be determined that at the outlet from the target the saturation temperature is 143.6°C. Therefore, if boiling is to be avoided the coolant temperature must be below 143.6°C at all locations.

The above preliminary description of the first proposed target will be used in the subsequent nuclear analyses.

Nuclear analyses of the design were carried out using the LAHET code system described above. The primary quantities of interest at this stage of the analysis are the neutron flux possible in the surrounding moderator, and the heating rate in the target components.

The total fluxes on the surface of the above target, and the energy deposited in the various target regions are given in Figures 3 and 4, respectively. The flux plots show the enhancement of the neutron flux achievable when the target is surrounded by a neutron multiplying material such as lead or beryllium, each of which has a significant n,xn production cross section.

The heat deposition calculation was carried out for each volume within the target. Thus, the heat deposition was determined for all sixteen frit-bed-frit-coolant combinations, and selected vessel walls. These values are used in the thermal analysis to compute the coolant and solid component temperatures.

The temperature of the coolant and metal components, and the cyclic thermally induced stress levels will be estimated as a function of the frit material. These estimates will be carried out for the first frit-bed-frit combination using tungsten frits. The largest amount of heat is deposited in this arrangement, and thus requires the highest coolant flow rates. Furthermore, it will be assumed that the beam spot at the entrance to the target is 4cms.x 4cms., and subsequently expands as it moves into the target. Thus, the entire heat deposited at this position appears in this relatively small volume, resulting in the highest power density. Finally, the solid volume involved must be further reduced to reflect the component porosity.

Table 4
Temperature Profile in Frit-Bed-Frit Structure

	Frit Type		
	W.	St. Steel	Be.*
#1 Frit Power			
Density (w/m^3)	5.51x10^9	3.23x10^9	1.0x10^9
Outlet Temp(°C)	43.0	42.0	41.0
Surface Temp(°C)	109.0	78.0	52.0
Bed Power			
Density (W/m^3)	8.98x10^9	8.98x10^9	8.98x10^9
Outlet Temp(°C)	56.5	55.2	55.0
Surface Temp(°C)	105.0	103.7	104.0
#2 Frit Power			
Density (W/m^3)	6.35x10^9	3.56x10^9	1.0x10^9
Outlet Temp(°C)	69.3	57.2	55.0
Surface Temp(°C)	129.2	96.0	67.0

* From estimated heat deposition

Based on the above assumptions regarding the beam and energy deposition, and assuming that the coolant inlet conditions are 40 °C and 5 bars, it is possible to determine the temperatures throughout the first element. These results are shown in Table 4. The results indicate that the tungsten frits are heated at a much higher rate than the stainless steel frits. The heat deposition in the tungsten frits is seen to be very similar to that deposited in the tungsten particle bed, while there is a much larger difference in the case using stainless steel frits. An even larger difference is expected in the case using beryllium frits. As a result of this relatively high heating rate in the all tungsten case the highest surface temperature is only 13° C below the saturation temperature. The corresponding temperature for the case using stainless steel frits is approximately 50°C below the saturation temperature, while the surface temperature in the case using beryllium frits is expected to be approximately 70°C below the saturation temperature. Based on this result it would be desirable to use stainless steel or beryllium frits. The alternative is to increase the target operating pressure, thus increasing the saturation temperature. An increase in pressure, however, would imply thicker vessel walls, which is not desirable.

An estimate was made to determine the thermal transient, and the implied thermally induced stress in the target components as the accelerator beam pulses on and off (approximately 10Hz and 50Hz). This analysis was carried out assuming that the accelerator beam reached full power instantaneously, and the subsequent temperature transient within the frits or particles was estimated by using published solutions to the heat conduction equation [Carslaw and Jaeger, 1986]. The resulting thermal stresses are enhanced by thermal-mechanical shock phenomena [Burgreen, 1962 and Conrad, 1994] which depend on the proton pulse duration and a characteristics target dimension.

In the particle bed the high thermal conductivity of tungsten (163 W/m-K), and the short conduction path (250 microns) ensure that the temperature rise from the particle surface to the center is no greater than approximately 44.8° K. This rise occurs very rapidly and implies a thermal stress of 7.0x10^3 psi., which is acceptably low. No stress related problem is expected in the particle bed.

Four frit materials were considered in this analysis, i.e., tungsten, stainless steel, beryllium, and aluminum. The heat deposition was estimated for the beryllium and aluminum

cases. In all these cases the thermal transient lasted longer than in the particle bed, because the conduction path is longer.

The equilibrium temperatures, and implied thermal stresses are given in Table 5.

Table 5
Temperatures and Stresses in Frits

Material	Equilibrium Temp.(K)	Stress (psi)
Stainless Steel	29.0	1.03×10^4
Tungsten	58.0	9.06×10^3
Beryllium	13.0	5.35×10^3
Aluminum	18.0	2.63×10^3

In order to evaluate these temperature and stress results it should be pointed out that they are applied cyclically. Thus, the stresses must be evaluated as inducing fatigue failures. With this criterion in mind, it is clear that stainless steel is not acceptable as a frit material, since cyclic stress levels of this magnitude are too high to ensure failure free operation. All the other cases result in acceptable stress levels. The high values for stainless steel are due to its poor conductivity, relatively high expansion coefficient and relatively high heat deposition. Thus, based on the transient analysis it is suggested that one of the three remaining candidate materials be used as the frit material.

DESCRIPTION OF SECOND TARGET CONFIGURATION

The second target configuration which satisfies all the requirements is derived from the two bed target configuration shown in Fig. 5. It consists of three target sections, separated by two flux trap sections. The target sections each consist of a particle bed configured in the direction of the proton beam with frits along two walls to admit the coolant. The pressure vessel forms the other two walls. Coolant enters the bed through one frit, flows through the bed at right angles to the beam, and exits through the other frit. Inlet and outlet plena for the coolant water are arranged above and below the frits. Cooling for the window and assorted structures to contain the particle beds is admitted through plena situated between the outer wall and that containing the particle beds. A beryllium flux multiplier surrounds the target volume. The current design of this component consists of a particle bed of beryllium spheres, cooled by heavy water. The coolant inlet pressure in the main target will be 6 atm, while in the case of the multiplier volume only approximately half that pressure will be required. The tungsten particles of the target volumes are 1 or 2 mm in diameter. This size represents a compromise between bed pressure drop, and maximum particle surface temperature. In the case of the beryllium particles in the multiplier a much larger range of particle sizes can be considered, since the conditions are less stringent. As in the first case, the target is expected to operate in a pulsed mode (10Hz.-60Hz.) with a proton beam energy of 3.6 GeV and a total beam power of 5 MW.

In this target arrangement the bulk of the proton energy is deposited in the tungsten particle bed. The structural walls in the direct path of the beam will all be subject to heating and will require cooling. These components consist primarily of the front window, and assorted walls to contain the particle bed. The most desirable materials for these components should have low values for NZ, ensuring low heating rates, and reasonably high operating temperature capability. The final selection will be made following the determination of heat rates.

All tungsten target volumes are 22cm wide and have varying thickness in the direction of the beam. The first section has a thickness of 7.5 cm, the second is 7.5 cm thick, and finally the last section is 39.5 cm thick. The flux multiplier surrounds the target volumes, and is 5 cm thick. All coolant passages are 2.5 mm thick, except the main coolant inlet and outlet plena, which are tapered, being 5 mm thick at the inlet end, and 2 mm thick at the other end. The tapered arrangement is necessary to compensate for the decrease in dynamic head of the coolant as it slows down, essentially coming to rest at the narrow end.

"Wing" type moderators will be placed adjacent to the target volumes, while "flux trap/back-scatter" type moderators will be placed adjacent to the flux trap volumes. These moderators can act as either "back-scatter" or "flux trap" moderators depending on which side of the moderator the flux is extracted. This will depend on the arrangement of the beam tubes. A maximum of sixteen beam tubes are possible with the currently configured target, i.e., two for each "wing" moderator (four/target implying a total of twelve), and two corresponding to each flux trap volume (one acting as a "back scatter" beam tube, the other acting as a "flux trap" beam tube for a total of four). It is assumed that all of the beam tubes will be arranged horizontally. Conceptually the moderator volumes are assumed to be rectangular with approximate dimensions of 10cmx10cmx5 cm. thick. The exact dimensions are dictated by the adjacent target or flux trap

size. All the beam tubes are assumed to be 7.5 cm in diameter.

In this target configuration it is also assumed that the proton beam is rectangular with a maximum foot print of 5 cmx20 cm. This beam spot size reduces to a minimum the possible heating and gas generation (due to proton interactions with the window material) in the window and should increase the reliability of the target.

The nuclear analyses of the proposed target design described above was carried out using the LAHET code system. The detailed geometry modeled in the LAHET/HMCNP simulations are shown in Figures 6 and 7 which represent slices through the target in the two planes perpendicular to the direction of the beam. Note that the particle beds, target structure, wing and flux-trap moderators and associated beam tubes are explicitly represented. The primary quantities of interest at this stage of the analysis are the neutron flux available to the users, and the heating rate in the target and moderator components.

In addition to generating preliminary estimates of the heating in the target for input to the thermal-hydraulic analyses, the nuclear analyses determined the fluxes and energy-dependent spectra in simulated beam tubes associated with various wing and flux-trap moderators: light water, liquid hydrogen, liquid deuterium, and liquid methane. Systems where the beam tubes and moderator were coupled, or decoupled by 1mm. cadmium liners were considered. Typical results are presented in Figures 8 and 9. Note that, even though the Cd liner reduces the thermal flux level it is expected that the time structure will have advantages for some experimental applications. This requires further evaluation.

The heat deposition calculation was carried out for each volume within the target. Thus, the heat deposition was determined for the window, three target volumes, structural components, flux multiplier, and cryogenic moderators.

The heat deposition rates were used to determine the metal and coolant temperatures. The target volumetric heating is highest in the first target volume, and drops off with distance into the target. The average heating in the three target volumes is approximately 95 kW/cm, 66 kW/cm, and 20 kW/cm respectively. Interestingly the heat deposition within each target volume is comparatively constant with distance along the proton beam. This characteristic is partially due to the proton energy chosen for the target (3.6 GeV), and makes the coolant distribution system less complicated and more reliable. A window made of aluminum would experience approximately one-half the heating as a stainless steel window (6.73 kW vs. 15.16 kW). The structural stainless steel walls, which separate the target particle beds from the flux trap volumes, experience varying degrees of volumetric heating. The front wall of the first target experiences a heat deposition of 13.21 kW, while the back wall of the third target experiences a heat deposition of 3.39 kW. However, it should be pointed out that except for the last wall, all other walls experience a volumetric heating rate of greater than 8 kW. Furthermore, the volumetric heat deposited in the beryllium flux multiplier is 18.41 kW, which implies a modest heat deposition, since it has a substantial volume. Finally, the heat deposited in the cryogenic moderators is comparatively low for the front target volumes, reaching a peak at the second target volume, and dropping off slightly at the third target volume. The average heat deposition in the three sets of "wing" moderators is seen to be 290 W, 742 W, and 705 W respectively. The total cryogenic refrigeration requirement for this target arrangement is seen to be 5.177 kW.

HEAT TRANSFER AND FLUID DYNAMICS ANALYSIS

In this section the temperature of the coolant, and metal components will be estimated. In addition the thermally induced stresses due to cyclic operation of the target will be estimated. In carrying out these estimates the beam spot sizes will be assumed to be 5 cm x 20 cm. The most intense heating per unit volume will occur in the front target, since the beam tends to expand as it enters the target, affecting a larger volume and thus reducing the volumetric heating per unit volume.

Based on the above assumptions regarding the beam size, energy deposition, and assuming that the coolant enters the target at 6 bars and 40°C, it is possible to determine the temperatures throughout the target. The coolant flow rate can be determined from the inlet conditions, the enthalpy rise, and the equation of state of water.

The mechanical design of the frits in this target is not as challenging as in the first particle bed target arrangement since they are not in the direct path of the proton beam. Their porosity is dictated primarily by the need to control the axial coolant distribution. Since the heat generation within each target is comparative constant in the axial direction the coolant flow distribution problem is comparatively simple.

The particle bed consists of tungsten particles with an appropriate coating to minimize oxidation of the tungsten.

The temperature profile within the target is given below in Table 6.

Table 6
Temperature profile within target bed

Power density (W/m^3)	1.4479×10^8
Coolant outlet temperature (°C)	80
Particle surface temperature (1000 micron) (°C)	93.5
Particle surface temperature (2000 micron) (°C)	115.7
Bed pressure drop (1000 micron) (N/m^2)	1.1121×10^5 [16.2 psi]
Bed pressure drop (2000 micron) (N/m^2)	5.1307×10^4 [7.45 psi]

The heating rate in the particles is modest compared to that of the first target design, since the beam spot is larger in this case. This lower heating rate leads to comparatively modest particle surface temperatures. In the case of both possible particle sizes the temperatures are significantly below the coolant saturation temperature. In the case of the smaller particle sizes (1000 micron) the bed pressure drop is marginally acceptable, and thus the larger particle size (2000 micron) will be adopted for the preliminary design.

An estimate was also made of the surface temperature of two possible window materials. Both aluminum and stainless steel were considered as possible candidates. In this analysis it was assumed that heat could only be removed from one face of the window, the other face being treated as an insulator. It was found that a coolant mass flow rate of 0.1 kg/s is required to remove the heat deposited in the window assuming an outlet temperature of 60°C. The following coolant conditions were assumed for this analysis, Table 7.

Table 7
Window cooling conditions

Coolant inlet pressure (Bars)	6.0
Coolant inlet temperature (°C)	40
Coolant outlet temperature (°C)	60
Mass flow rate (kg/s)	0.1
Coolant velocity (m/s)	0.2

The above conditions do not allow for a sufficiently low film drop in the case of aluminum, and thus the coolant velocity must be increased to ensure an acceptable window surface temperature. An increase in the coolant velocity to 10 m/s, through the same 2mm thick coolant passage behind the window will have the desired effect. In this case the mass flow rate will be 4.4 kg/s, the coolant outlet temperature will drop to essentially 40.5°C, and the aluminum surface temperature will be 62.2°C. These temperatures are very modest, and should be acceptable for operation with 6061 series aluminum. In the case of stainless steel the heating rate is approximately twice as high, implying proportionately higher temperatures. However, stainless steel can operate safely at higher temperatures, with the coolant saturation temperature being the limiting value. If it is found that 10 m/s is too high a velocity, since it requires a high pressure drop, it can be reduced to approximately half that value with aluminum without compromising the operation.

The cyclic stresses induced in the aluminum window were estimated to be 3820 psi, which is within the acceptable limit for aluminum. A more detailed analysis will have to be undertaken if aluminum is chosen for the final design.

CONCLUSIONS

The following conclusions can be drawn from this study:

1) It is possible to generate a total neutron flux of $\sim 10^{15} n/cm^2$-s using the proposed target designs.

2) Two particle-bed-based target arrangements were discussed and analyzed:

   - Particle beds arranged at right angles to the direction of the proton beam to ensure minimum bed thickness, but with frits in the beam. The selection of tungsten particles 500 microns in diameter, and frits made of beryllium 2mm - 3mm. thick ensures that no fatigue failures are likely to occur, that the coolant is always well below the saturation temperature at the 5 bar operating pressure, and that the melt temperatures of the components are well above the operating temperature.

   - Particle beds arranged along the direction of the proton beam. In this case the frits are out of the direct beam, but the beds tend to be thicker, requiring larger particle diameters to reduce the

bed pressure drop. The selection of tungsten particles 2000 microns in diameter and frits made of stainless steel situated outside of the proton beam has the advantage that the particle bed absorbs most of the volumetric heating. The other advantages from the above target also apply.

3) The question of tungsten oxidation by free oxygen generated by radiation-induced coolant dissociation needs to be addressed.

4) A back-up cooling system for the target to guard against under-cooling will rely on the large thermal margin and the efficient heat transfer possible from a particle bed.

5) Thermal-mechanical shock enhancement of the thermal stress needs to be evaluated for windows and internal structural components.

REFERENCES

R. E. Prael, "LAHET Benchmark Calculations of Differential Neutron Production Cross Sections for 113 MeV and 256 MeV Protons", LA-UR-89-3347, Los Alamos National Laboratory (September, 1989)

R. E. Prael, "LAHET Benchmark Calculations of Neutron Yields from Stopping-Length Targets for 113 MeV and 256 MeV Protons", LA-UR-90-1620, Los Alamos National Laboratory (May, 1990)

G. J. Russell, "APT Santa Fe Design Review", March 1-4, 1993.

M. Todosow, "APT Santa Fe Design Review", March 1-4, 1993.

S. Sitaraman," MCNP: Light Water Reactor Critical Benchmarks", NEDO-32028, General Electric Nuclear Energy, March, 1992.

D. Whalen, et al, "MCNP: Neutron Benchmark Problems", LA-12212, Los Alamos National Laboratory, November, 1991.

J. C. Wagner, et al,"MCNP: Criticality Safety Benchmark Problems", LA-12415, Los Alamos National Laboratory, October, 1992.

D. Burgreen, "Thermoelastic Dynamics of Rods, Thin Shells, and Solid Spheres", Nuclear Science Engineering, 12, p. 203, (1962).

H. Conrad, "On Elastic Stress Waves in Targets", European Spallation Source Report, Forschungszentrum, Jülich, ESS 94-5-T (1994).

H. S. Carslaw and J. C. Jaeger, "Conduction of Heat in Solids, 2nd Edition", Clarendon Press, Oxford (1986).

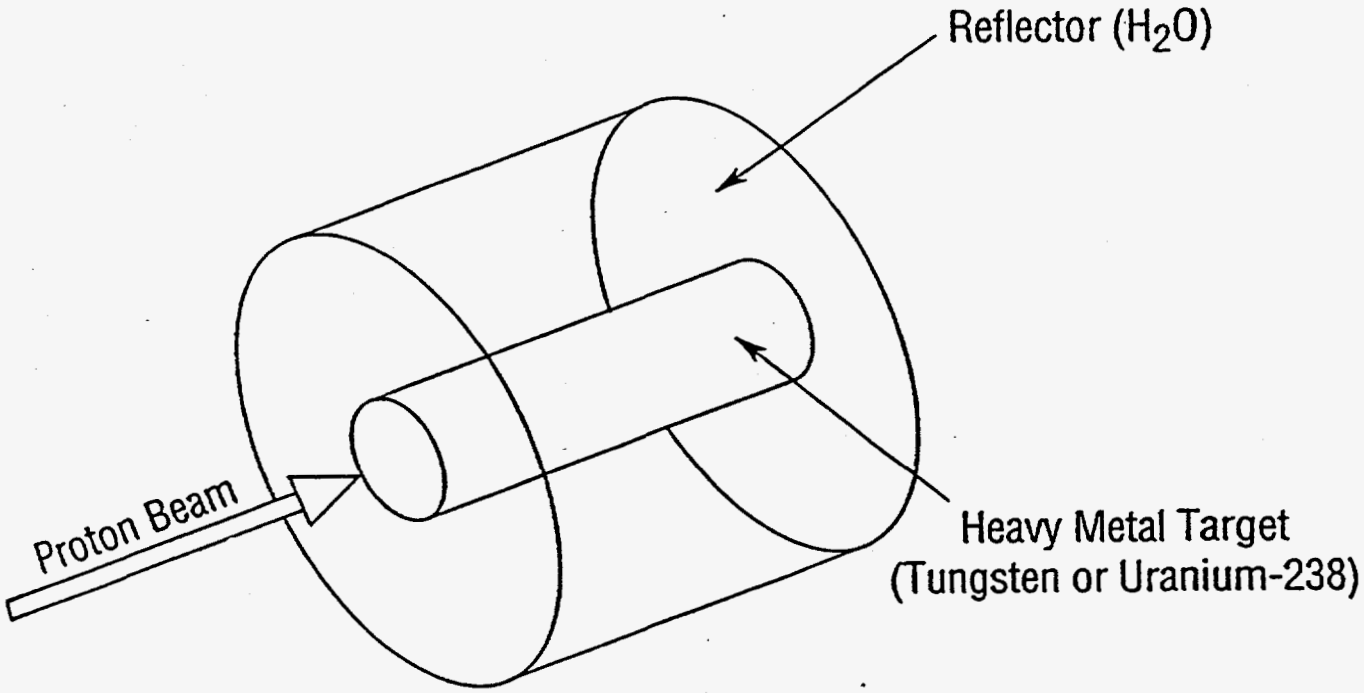

Figure 1. Schematic Representation of Heavy Metal Target Surrounded by a Reflector

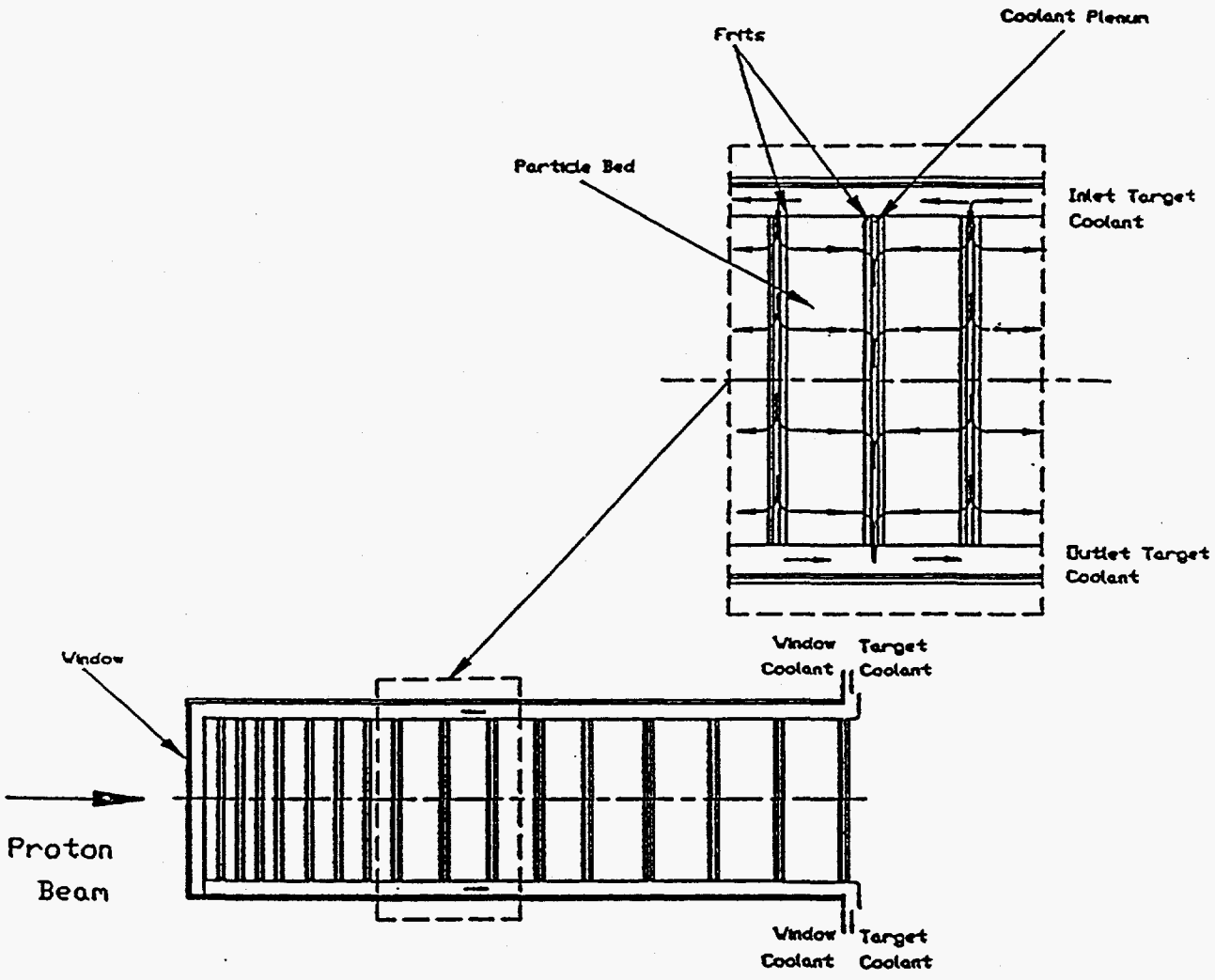

Figure 2. Schematic Illustration of Spallation Target Based on Particle Bed Technology

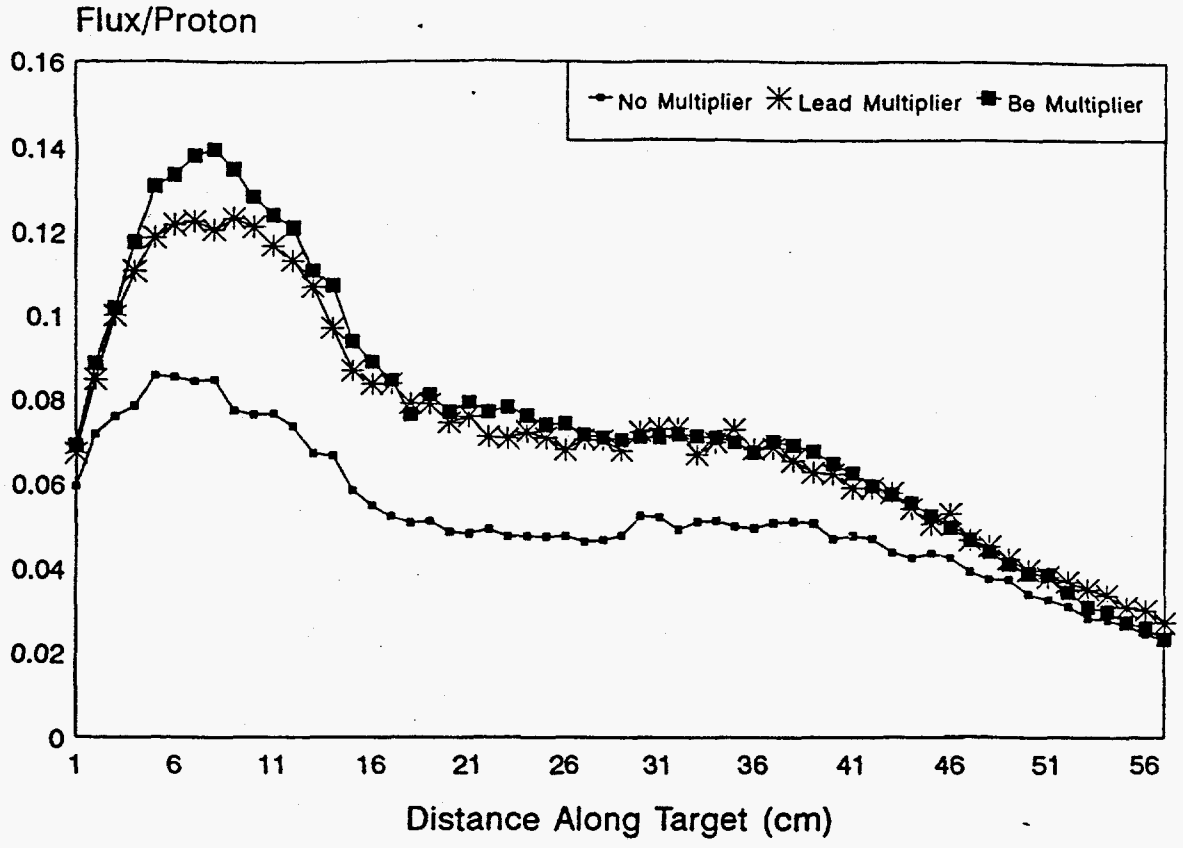

Figure 3. Total Fluxes on Surface of Target

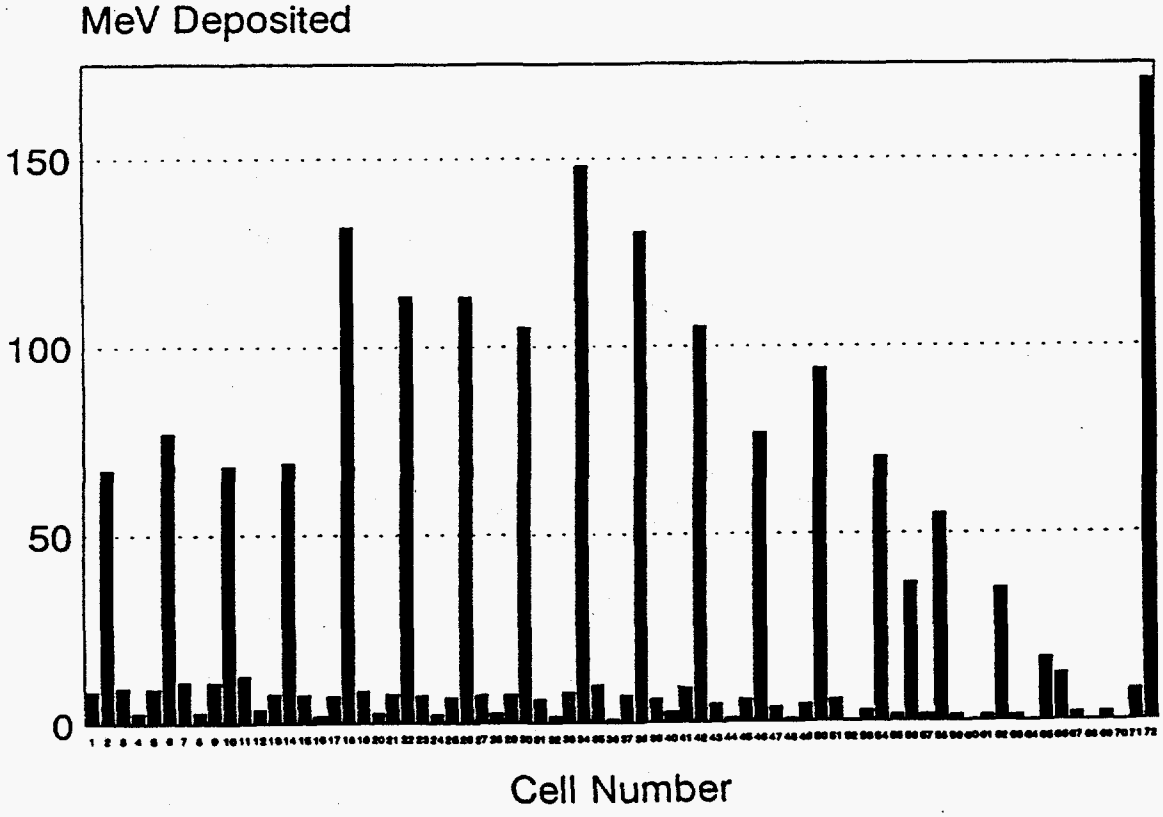

Figure 4. Energy Deposition from LAHET (E>20MeV)

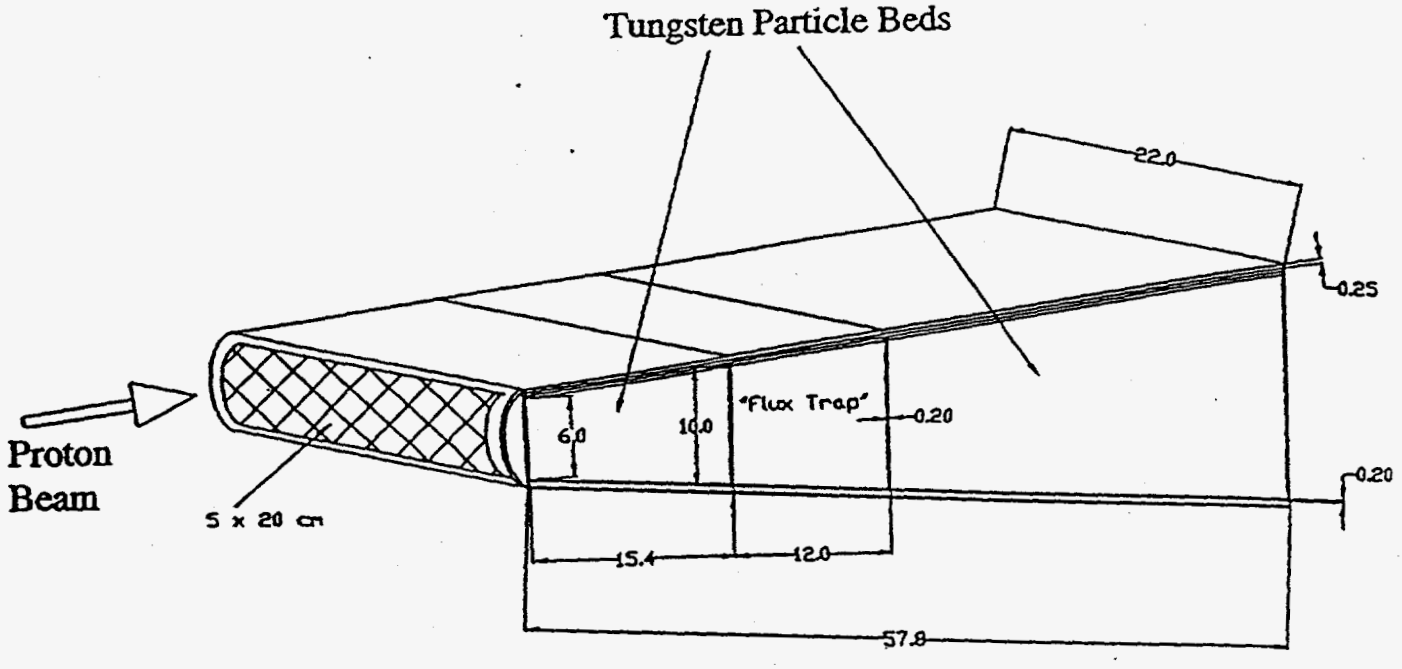

Figure 5. Two Bed Target

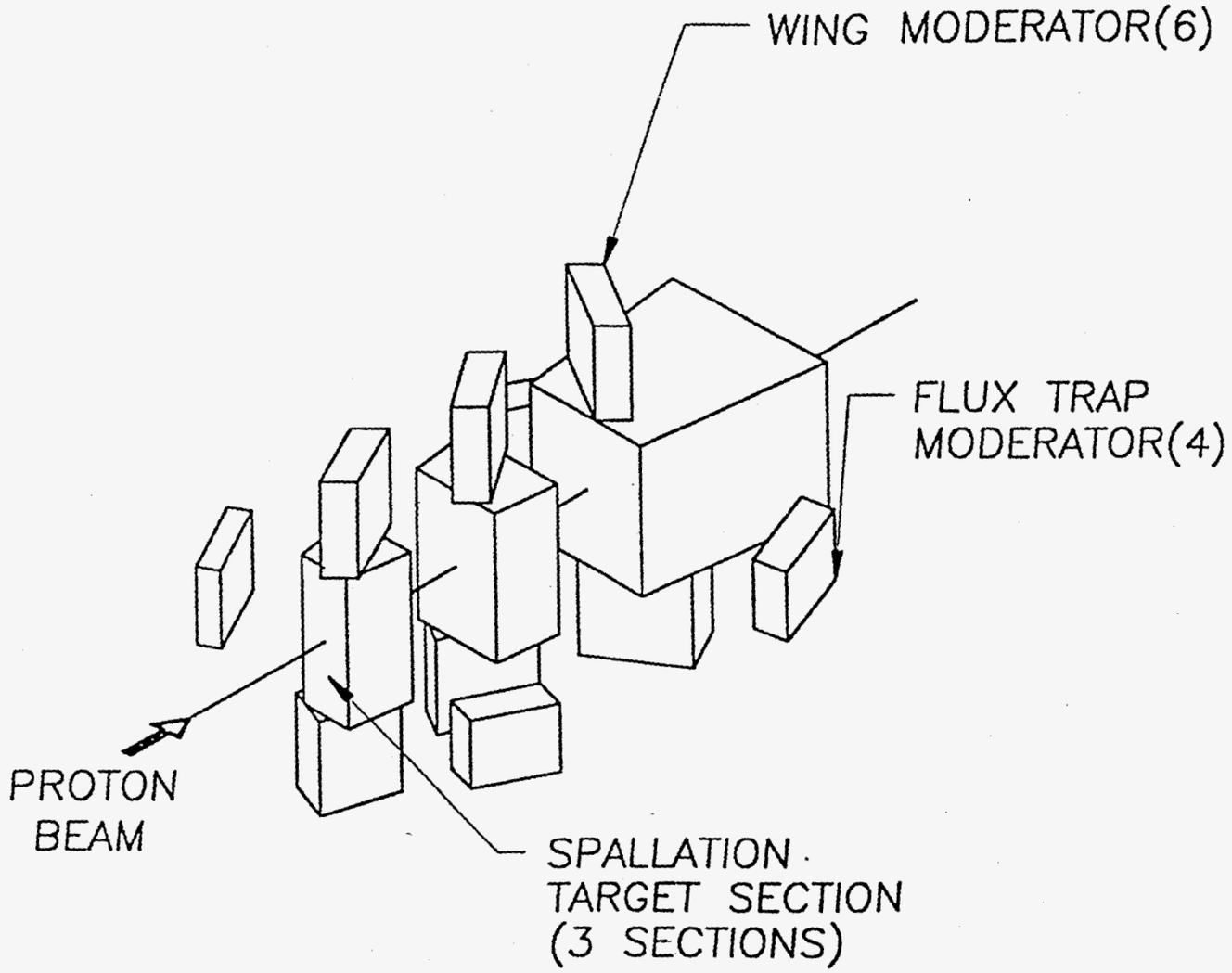

Figure 6. Spallation Target and Moderator Configuration

```
 04/06/94 09:23:41
     PBSNSX4: 3-SECTION W
 TARGET: 3.6GEV; SS-FRITS; HWTR
 MOD; Be MULT
probid =  04/06/94 09:18:38
basis:
(  .000000, 1.000000,  .000000)
(  .000000,  .000000, 1.000000)
origin:
(      .00,      .00,      .00)
extent = (    70.00,    70.00)
```

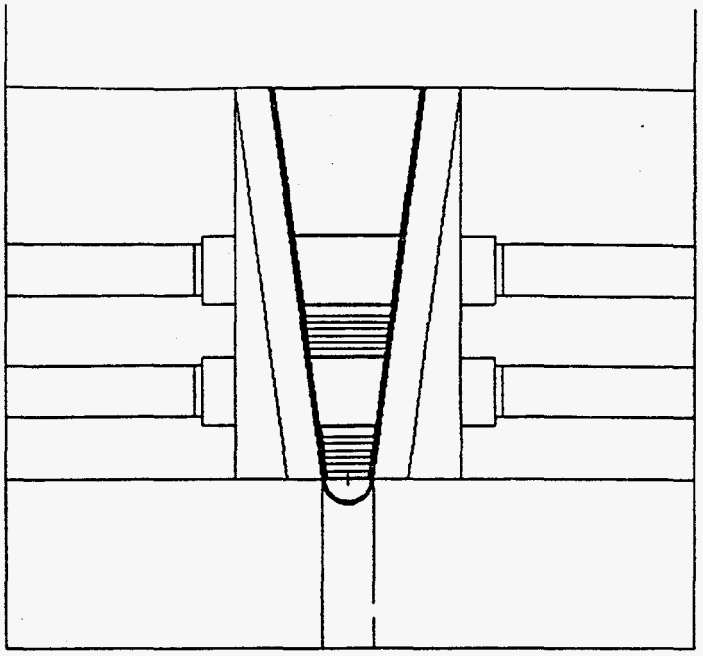

Figure 7a. Flux Trap Moderators and Beam Tubes Opposite "Void Gaps"

```
 04/06/94 09:23:00
     PBSNSX4: 3-SECTION W
 TARGET; 3.6GEV; SS-FRITS; HWTR
 MOD; Be MULT
probid =  04/06/94 09:18:38
basis:
( 1.000000,  .000000,  .000000)
(  .000000,  .000000, 1.000000)
origin:
(      .00,      .00,      .00)
extent = (    70.00,    70.00)
```

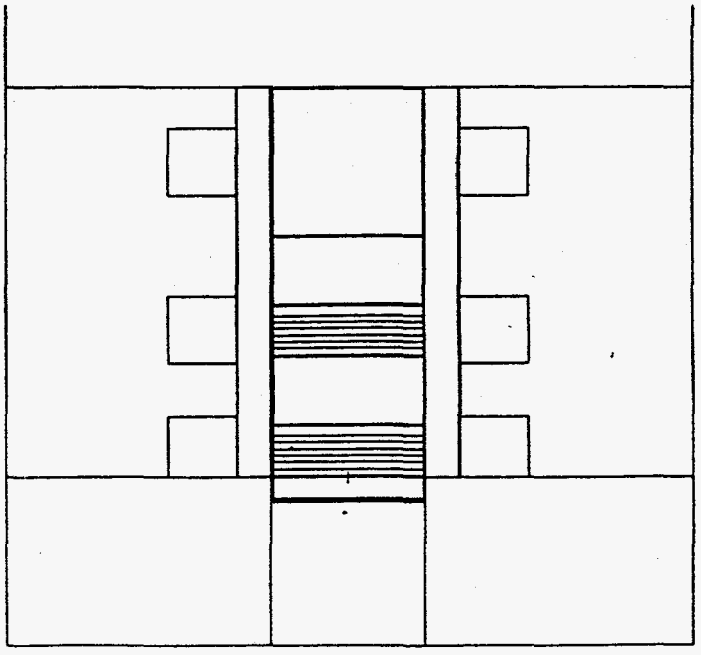

Figure 7b. Wing Moderators Above and Below the Three Particle Beds

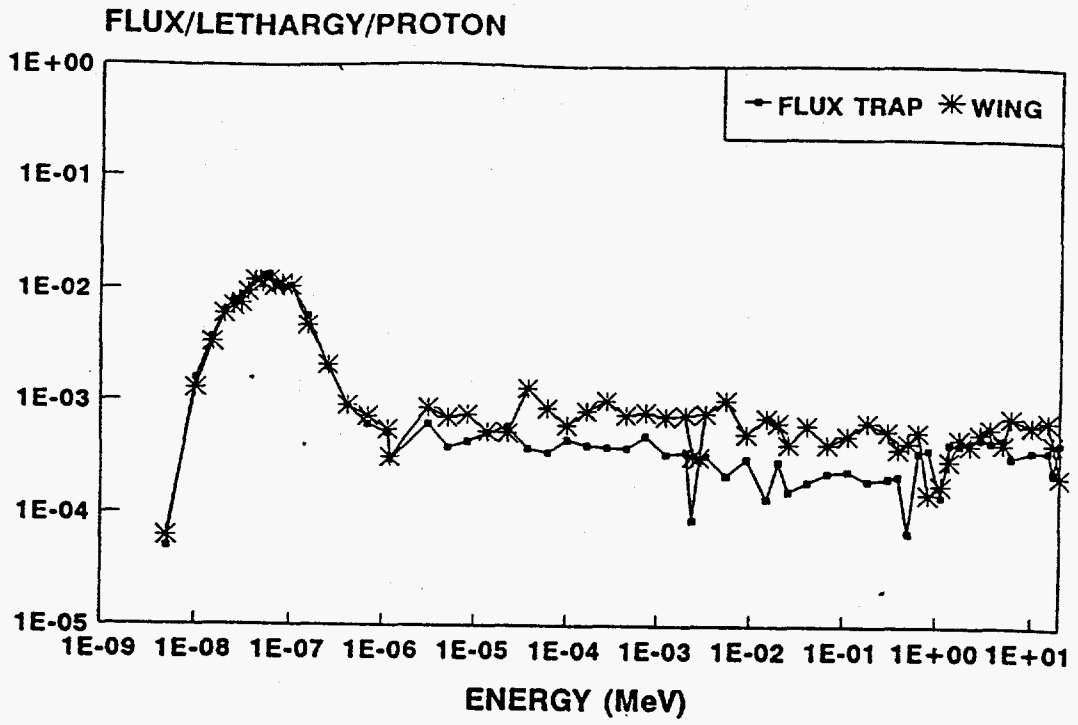

Figure 8. Beam Fluxes for Light Water Flux Trap & Wing Moderators

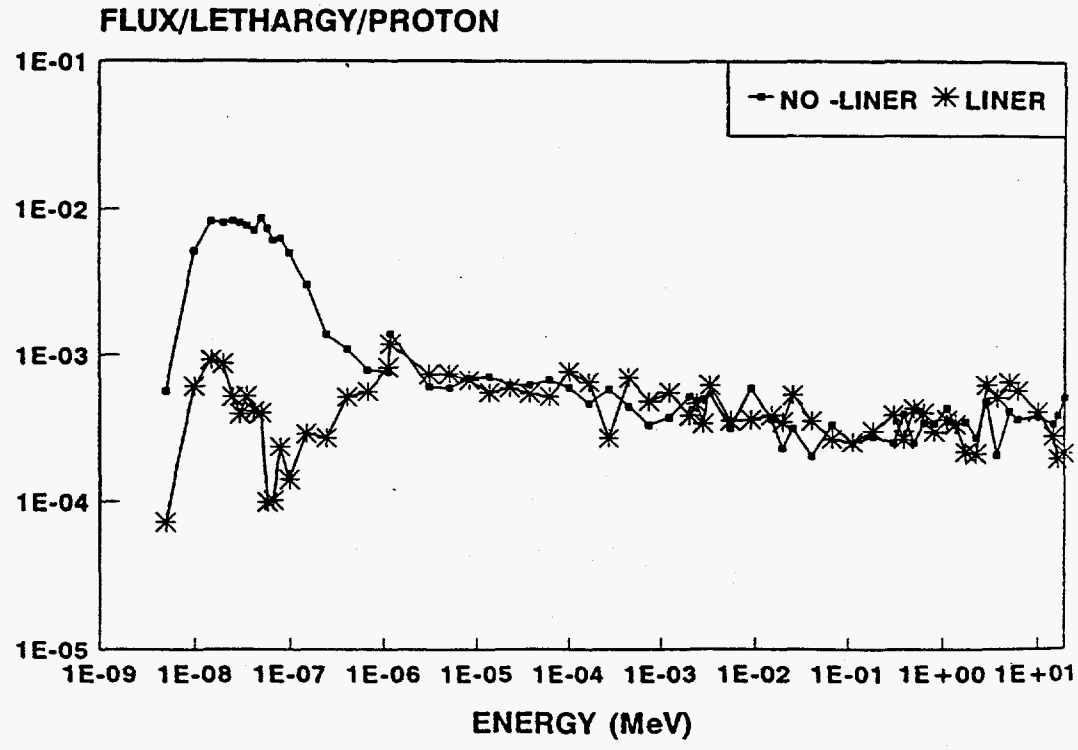

Figure 9. Effect of Cadmium Linder on Beam Tube Flux Spectra